Journal of Achievements in Materials and Manufacturing Engineering
VOLUME 37
ISSUE 2
December
2009

Microstructure and properties of CuNi2Si1 alloy processed by continuous RCS method

J. Stobrawa [a,b,*], Z. Rdzawski [a,b], W. Głuchowski [a], W. Malec [a]
[a] Non-Ferrous Metals Institute, ul. Sowińskiego 5, 44-100 Gliwice, Poland
[b] Division of Materials Processing Technology, Management and Computer Techniques in Materials Science, Institute of Engineering Materials and Biomaterials, Silesian University of Technology, ul. Konarskiego 18a, 44-100 Gliwice, Poland
* Corresponding author: E-mail address: jerzy.stobrawa@imn.gliwice.pl

Received 15.09.2009; published in revised form 01.12.2009

Properties

ABSTRACT

Purpose: Precipitation strengthened copper constitutes a group of functional and structural materials used where combination of high electrical conductivity with high strength is required. A growing trend to use new copper-based functional materials is recently observed world-wide. Within this group of materials particular attention is drawn to those with ultrafine grain size of a copper matrix.
Design/methodology/approach: This study was aimed to investigate mechanical properties and microstructure in strips of age hardenable CuNi2Si alloy processed by continuous repetitive corrugation and straightening (CRCS). Tests were performed with quenched (900°C/1hour/water) or annealed (650°C /1 hour) 0.8 mm thick strips using original die set construction (toothed rolls and plain rolls set) installed in tensile testing machine. The changes of mechanical properties (HV, ultimate tensile strength, 0.2 yield strength) as well as microstructure evolution versus number of deformation cycles were investigated. The microstructure was investigated by optical and electron microscopy (TEM and SEM equipped with EBSD).
Findings: The obtained strengthening effects and observed microstructure changes have been discussed basing on the existing theories related to strengthening of ultra fine grained copper based materials.
Practical implications: The CRCS process effectively reduced the grain size of CuNi2Si1 alloy strips especially for annealed material, demonstrating the CRCS as a promising new method for producing ultra fine grained metallic strips.
Originality/value: The paper contributes to the mechanical properties of precipitation strengthened ultra fine grained copper - chromium alloy strips obtained by original RCS method and to the microstructure evolution.
Keywords: Severe plastic deformation; Ultra fine grained material; Mechanical properties; Electron microscopy; Metallography

Reference to this paper should be given in the following way:
J. Stobrawa, Z. Rdzawski, W. Głuchowski, W. Malec, Microstructure and properties of CuNi2Si1 alloy processed by continuous RCS method, Journal of Achievements in Materials and Manufacturing Engineering 37/2 (2009) 466-479.

1. Introduction

A growing trend to use new technologies for production of ultrafine grained materials has been recently observed. The structure of ultrafine materials consists of components, which have at least one dimension within the range below 100 nm [1]. Important part of this kind of materials is represented by precipitation strengthened copper alloys with ultrafine grain size (UFG) of copper matrix, which exhibit higher mechanical properties than microcrystalline copper alloys. To produce bulk copper materials of ultrafine grain sizes, powder metallurgy techniques [2-7] are being used. Severe plastic deformation methods seem to be promising techniques for those applications. Equal–channel angular pressing (ECAP) [7-11] is very popular which might be used for processing of steel or nonferrous materials, including copper, aluminum [1], nickel-titanium [8], magnesium [9] alloys. It was proven that deflection of the channel in the horizontal part leads to significant increase in deformation intensity at the first pass of the sample thorough the ECAP channel [10-11]. However, proper handling of friction conditions

a)

b)

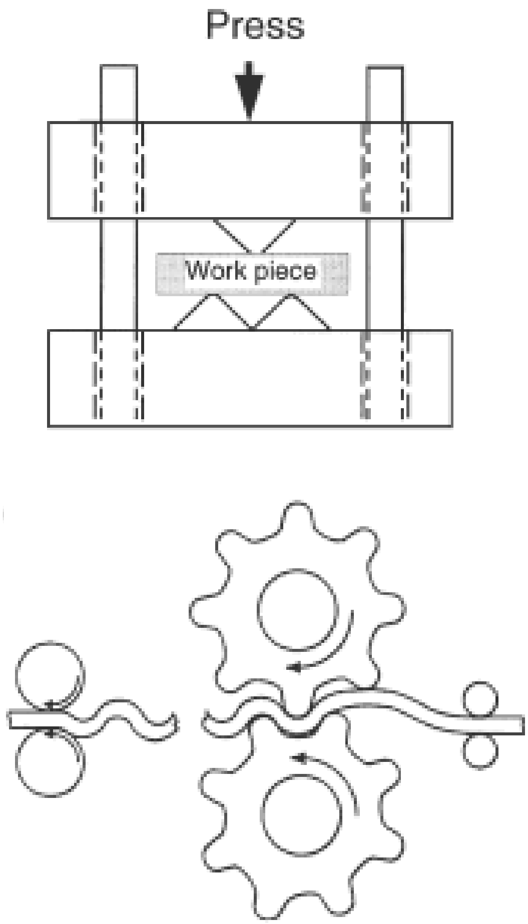

Fig. 1. RCS method scheme a) discontinuous, b) continues [19]

conditions to the partial contact conditions at the beginning of deformation. It is very important for proper understanding of the during processing is difficult. Process simulations reveal that deformation mode changes from extrusion in the full contact deformation mechanics and determining the load requirements for the ECAP with the larger specimen for industrial applications [12]. The other SPD techniques are hydrostatic extrusion (HE) [13] and high-pressure torsion (HPT) [14-16]. In this process the formation of sub-grain structure is seen after deformation where cells show broad boundaries of a diffuse dislocations arrangement, which transform to high angle grain boundaries at higher strains. The sub-grain interiors also contain irregularly-shaped dislocations. For this reasons the effect must be explained by movements of dislocations (rearrangements of dislocations), where dislocations continuously build up and form new boundaries as the deformation increases [17].

All of these methods are not conducted continuously, and they seem to be impractical for manufacturing plate – shaped ultrafine grained materials. Recently, a new technique, i.e. repetitive corrugation and straightening (RCS) [18-20] has been developed for production of UFG microstructures in plate– shaped products. In the RCS process (Fig. 1), a work-piece is repetitively corrugated and straightened without significant changing the cross-section geometry - and what is very important - this process can be easily adapted to a large – scale production.

The main objective of this work was to study the changes of mechanical properties as well as microstructure evolution versus number of deformation circles of CuNi2Si1 strips processed with CRCS method.

2. Process simulation

Continuous corrugation and straightening is a dynamic process, thus its simulation is difficult. Therefore, to simplify the calculations, a static simplified analogical model of copper strip processing to the corrugation and straightening process is used. This procedure has been applied also in this work. The main objective was to draw up the deformation map on the strip cross sections after corrugation for established corrugation tool geometry.

Copper strip corrugation process has been simulated with finite elements method using bilinear elastic – plastic material model being characterized by:

- Young's modulus $E = 1.25 \times 10^{11}$ Pa
- Elastic modulus of volume $G = 5.3 \times 10^{10}$ Pa
- Poisson ratio $\nu = 0.33$
- Yield point $YP = 35 \times 10^{6}$ Pa
- Density $\rho = 8900$ kg/m^3

In the presented model the strip is corrugated with a toothed bar (Fig. 2). Bottom toothed bar is fixed. It is fixed in a stable position with stable pivot bearings. The upper toothed bar and the strip can shift vertically. Used force to the upper toothed bar causes strip corrugation.

Dimensions of corrugated strip are presented in Table 1

Table 1.
Dimensions of simulated strip

Length	170 mm
Width	5 mm
Thickness	1 mm

The reaction between strip and toothed bars was simulated with the assumed adequate boundary conditions. Nonlinear numerical calculations were conducted with ANSYS computer system. The complete model data and obtained calculation results (displacement maps, deformation maps, stress maps, deformation energy density maps) could be found in work [19]. Some examples of calculation results are presented below (elastic deformation map Fig 3, plastic deformation map Fig. 4, total deformation map Fig. 5). We can conclude that for copper alloys, after one corrugation pass, the local deformation could be close to the 0.3. After straightening this value could be increased to 0.6. Deformation rate changes in cycles. For its homogeneity the corrugation and straightening process (with controlled dislocation of toothed bars) needs to be repeated three times.

The obtained simulation results were used when defining the structure of a prototype device for repetitive corrugation and straightening of cooper and copper alloys strips. It was also used for determination of initial process parameters for obtaining sub-micro or nanostructures in these materials. Microstructure investigation results of electrolytic copper initial test processing, which correspond to the simulation results, are presented in Fig. 6.

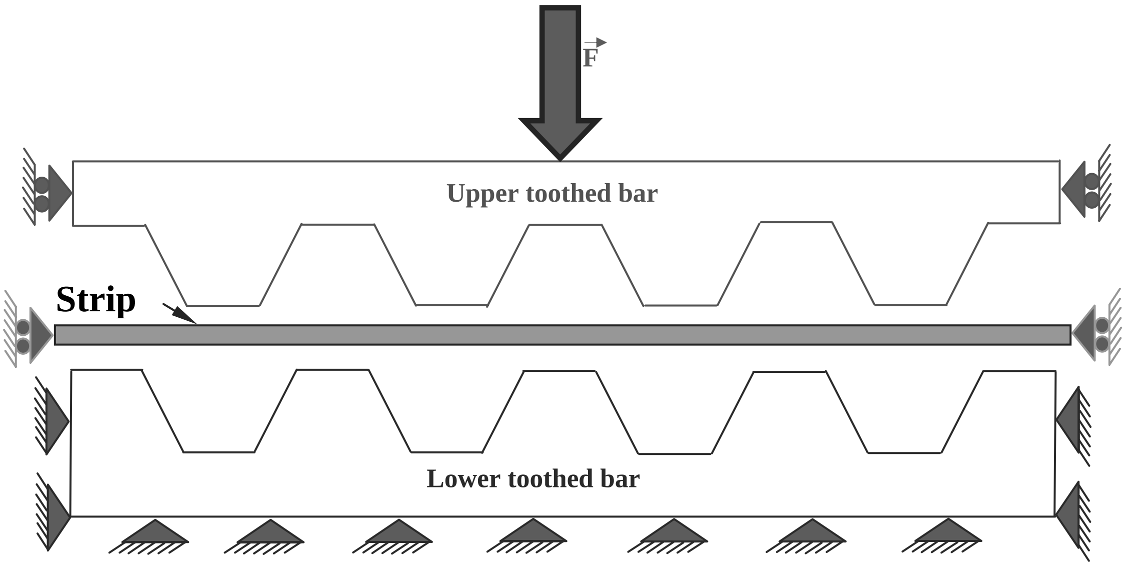

Fig. 2. Diagram of strip corrugation with toothed bars

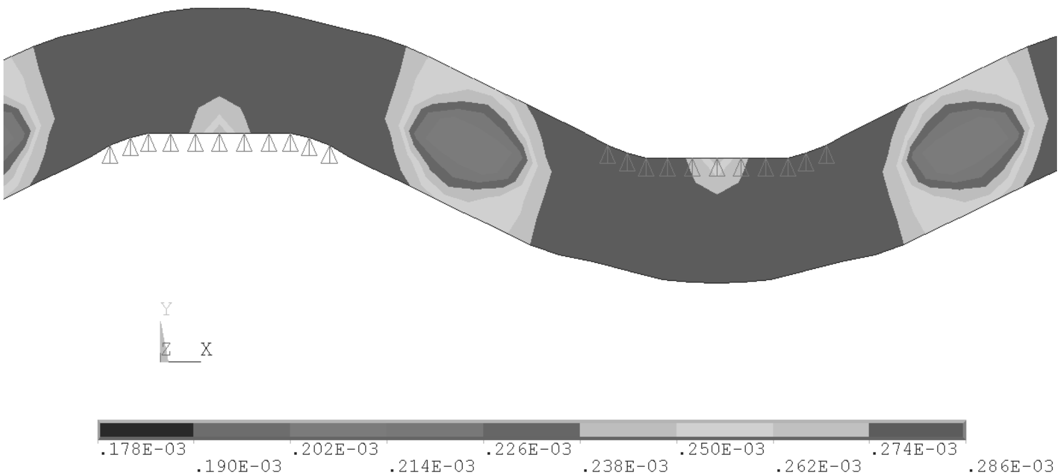

Fig. 3. Reduced elastic deformation map

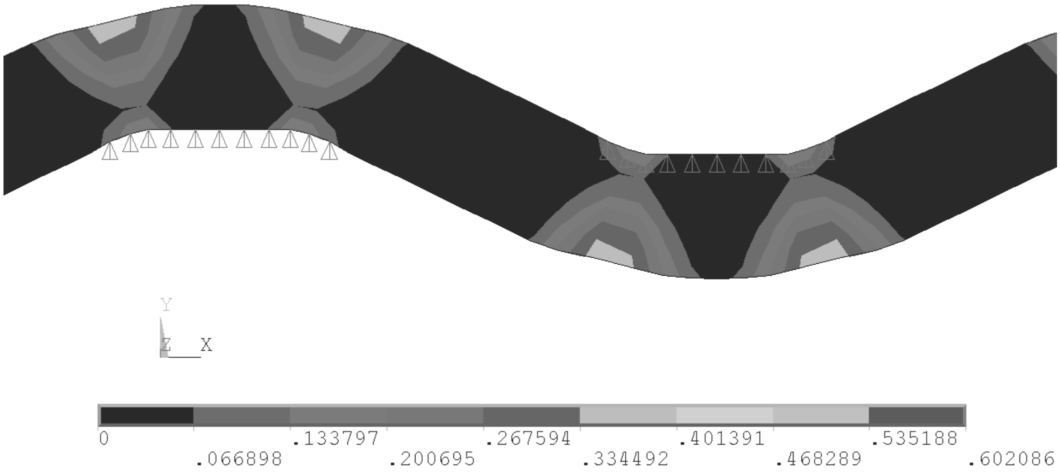

Fig. 4. Reduced plastic deformation map

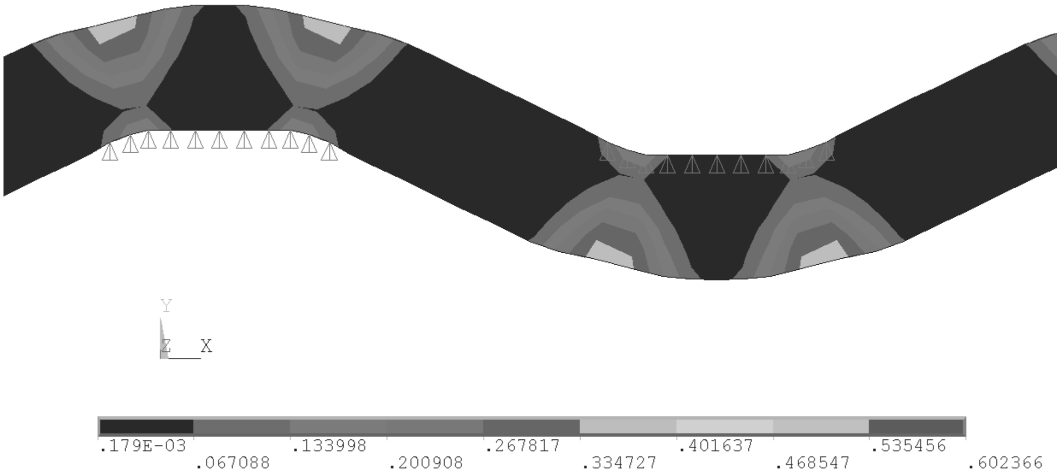

Fig. 5. Reduced total deformation map

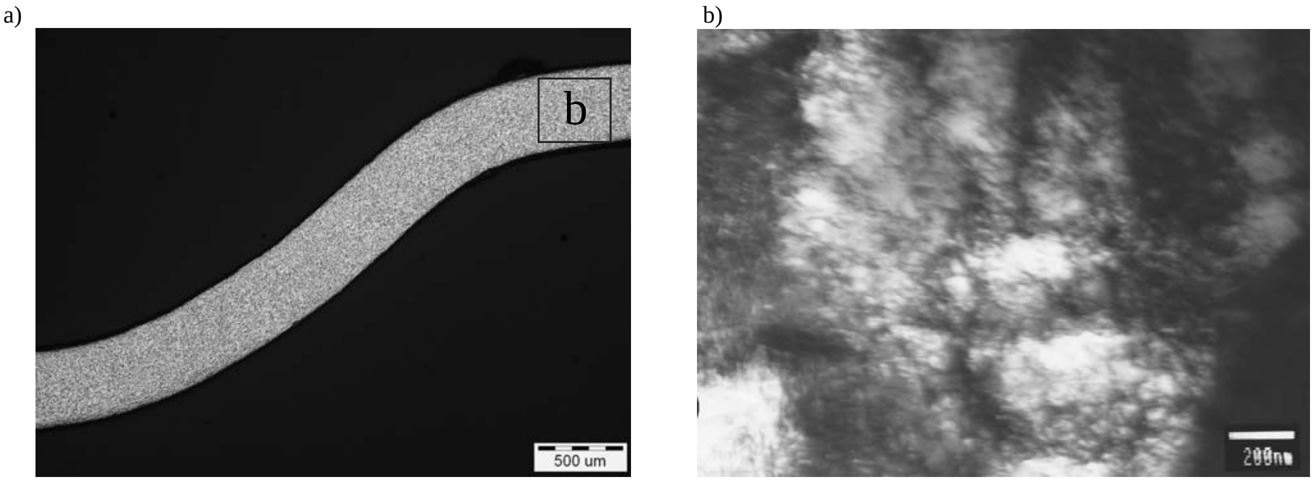

Fig. 6. Microstructure of electrolytic copper strip processed with RCS method a) optical microscopy and b) TEM image of the marked area

3. Experimental procedure

Precipitation hardened copper alloy with addition of 2%Ni and 1% Si (CuNi2Si1) was used in investigation, prepared by melting and alloying in an open-air induction furnace, followed by casting into 130x170 mm mould. Blooms were hot rolled down to strip thickness of 3 mm. After surface brush cleaning the strips were cold rolled down to thickness 0.8 mm. Strip samples 1000 mm (length) x 20 mm (width), quenched in water from 900^{o}C or annealed at 650^{o}C for 1 hour, were prepared for tests.

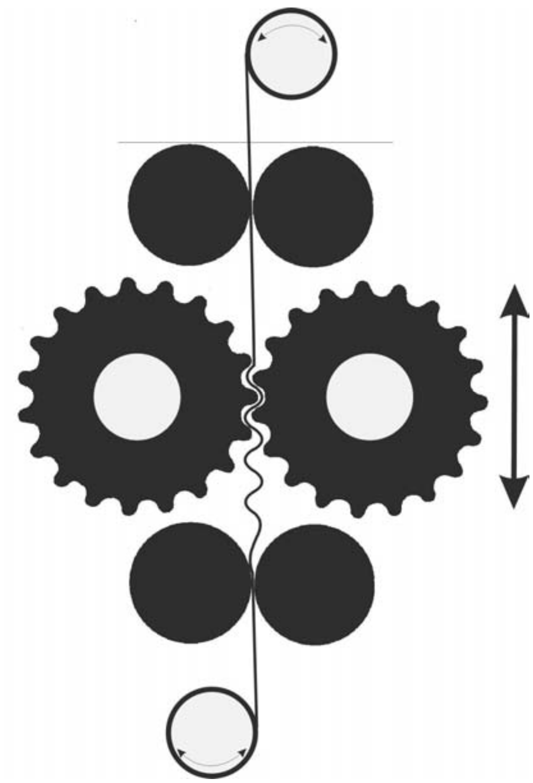

Fig. 7. Diagram of rolling set for CRCS method

Continuous repetitive corrugation and straightening process was conducted by drawing of a strip through a set of toothed rolls (corrugation) and plain rolls (straightening). All rolls were assembled in a rolling set giving a possibility to control the clearance of rolling gap (Fig. 7). This set was installed in tensile testing machine INSTRON (Fig. 8), giving a possibility for a local strip deformation (true strain) of about 0.6 in one pass. During the test the investigated strips were fixed while the set of rollers was shifted along with the tensile test machine cross-bar travelling. The process was conducted in both directions. 6, 12, 24 and 34 cycles of continuous repetitive corrugation and straightening were carried out. Thickness of strips after the process was reduced to 0.7 mm. The microstructure characterization was carried out on samples of initial material and after 34 cycles, using electron backscattered diffraction (EBSD) pattern measurement and transmission electron (TEM) microscopy. It was done on surfaces perpendicular to transverse directions. The EBSD measurements were carried out in a scanning electron microscope of field emission type (Inspect F) equipped with OIM (Orientation Imaging Microscopy) system. The Transmission electron microscope investigations were made using JEOL (JEM 2000 FX). The scanning parameters were set in such a way that a grain boundary was defined when the disorientation between adjacent measurement points was higher than 6^{o}. In the results the grain size determined by EBSD was smaller than the actual value. To provide accuracy, these results were used in combination with TEM to determine the correct value. Mechanical properties of strips after 0, 6, 12, 24 and 35 cycles were investigated in tensile tests using INSTRON machine. The tensile test of each sample was carried out at the initial strain rate of 1.0×10^{-3} s^{-1} in room temperature.

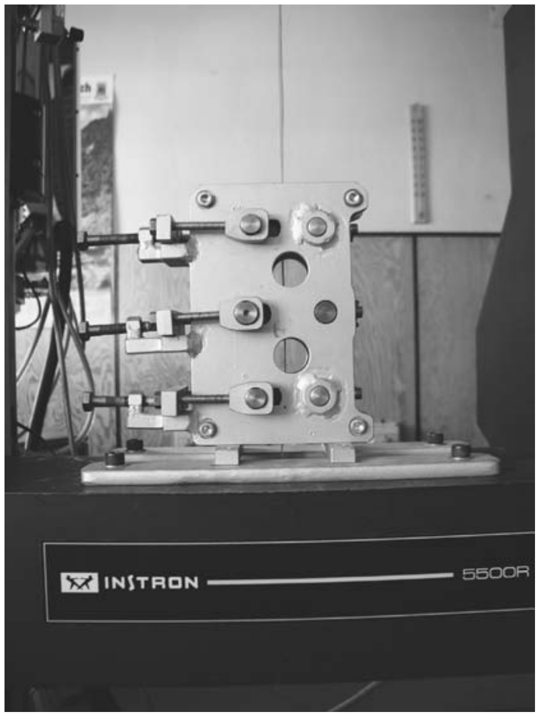

Fig. 8. CRCS rolling set installed in testing machine

4. Mechanical properties

The study of the mechanical properties (tensile and hardness tests) was conducted on CRCS samples that were quenched at 900^{o}C for 1 hour or annealed at 650 ^{o}C for 1 h before corrugation and strengthening. The results of these tests versus number of deformation passes are shown in Fig. 9.

The initial CuNi2Si1 samples showed large ductility. Work hardening in the CRCS process caused a large decrease in ductility of the sample and increase of strength.

a)

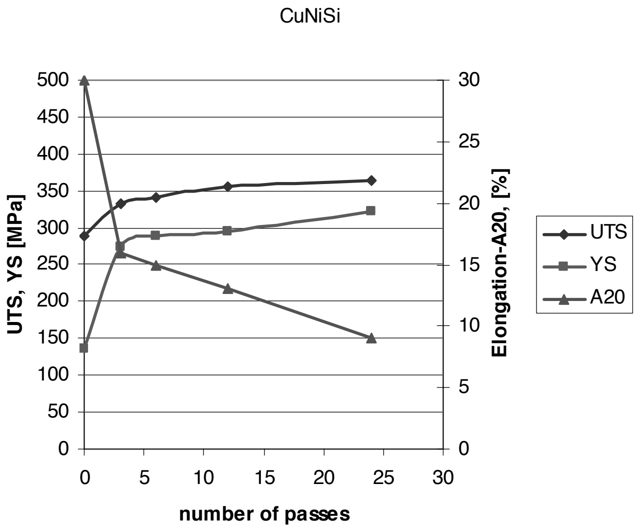

b)

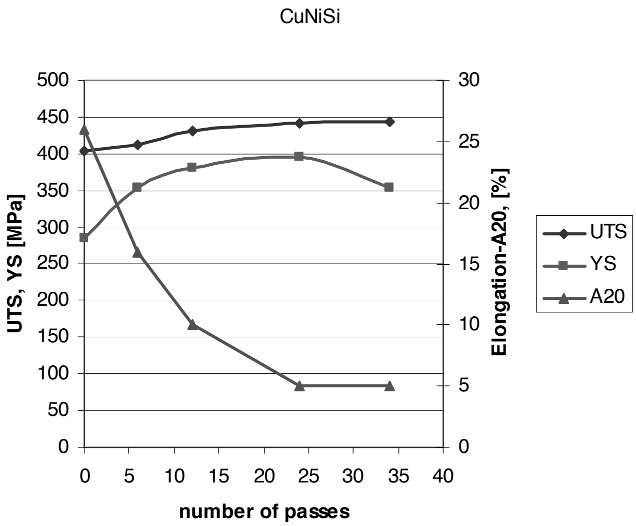

Fig. 9. Changes of mechanical properties of CuNi2Si1 strip during CRCS processing of a) quenched strip and b) annealed strip

The values of strength characteristics of CuNi2Si1 strips such as yield strength and ultimate tensile strength increased by a factor 1.4 and 1.1, respectively for both initial material types. Maximal strengthening effect was achieved after 24 cycles of CRCS process. Further deformation of initially annealed samples caused decreasing of strengthening factors to the values of about 1.2 and 1.1, in the result of UTS decreasing after 34 deformation cycles.

The ductility of the samples expressed by relative elongation decreases from about 30% to about 10% for the quenched material and from 26% to about 5% for the annealed one.

These results indicated complex deformation pattern and a possibility to start new slipping systems, thus the deformation resistance during CRCS deformation was lowered.

5. Microstructure

Investigations with a SEM equipped with electron back scattered diffraction system provided possibilities for precise identification of crystal structure of investigated materials via its orientation components. Grain boundaries, twin boundaries and precipitates are clearly defined in this method. By contrast, the etched secondary electron microstructure image does not show the same level of details.

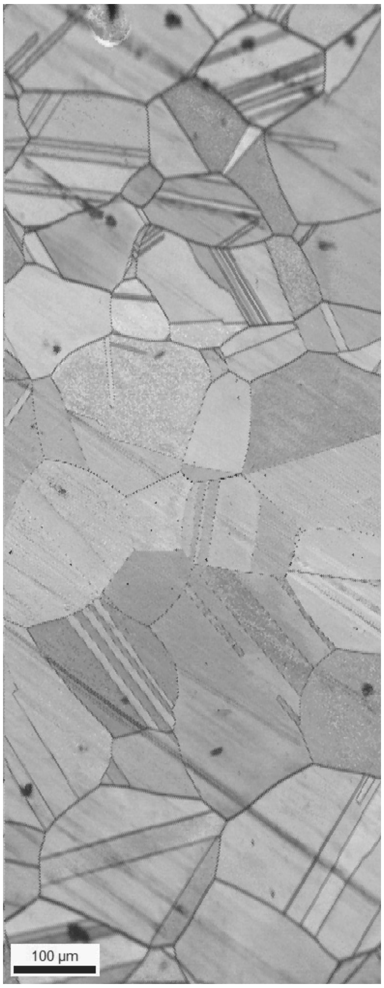

Fig. 10. Image quality map (IQ map of initial quenched strip)

Figure 10 presents image quality map (IQ map) of an initial sample of quenched strips. IQ map shows the brightness of the diffracted bands. Any area that produces poor patterns such as grain boundaries, poorly prepared phases, and surface damage will show up dark fields. In our case the bright grains in this image are the grains of supersaturated CuNi2Si1 solid solution. Nearly 95% of partition points were indexed. The measured average grain diameter was about 170 μm, twin fraction: 0.28 and fraction of twinned grains about 0.62. Grain map for this case is shown in Fig. 11. In this map all the grains are colour-coded according to the size (see legend below), Neighbouring pixels that have maximum misorientation of 5° are grouped together as grains while the twin lamellae are not identified as intragranular features.

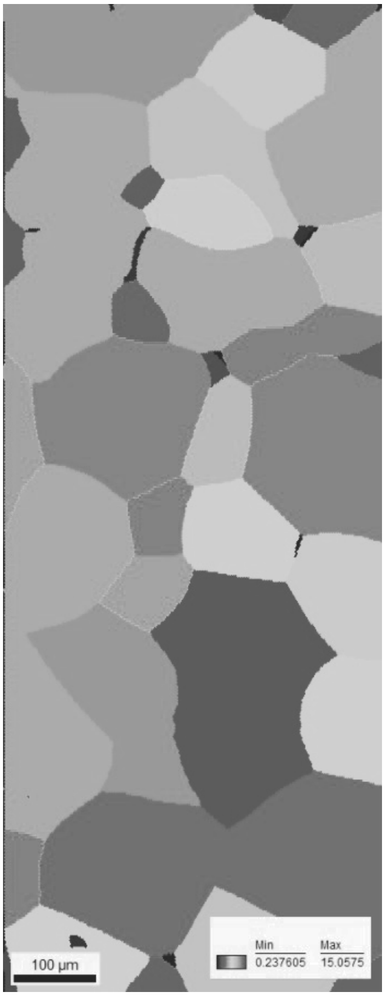

Fig. 11. Grain map of initially quenched strip

Grains size distribution for such case is shown in Fig. 12. Inverse Pole Figure (IPF) map shows the crystal direction parallel to the specimen while normal using the colour-coding according to the unit triangle. In many of the grains fcc twin lamellae can be recognised, and orientation in most of them is close to <101> (Fig. 13). In Fig. 14 histogram of misorientation angle of grain boundaries is presented. We can see that the majority of the grain boundaries before deformation were of high angle type and about 50% of them were of about 60°.

Microstructure refinement was observed after CRCS process for CuNi2Si1 alloy strips (Figs. 15-17). While in the initial (quenched) strips average grain diameter was about 170 μm the average grain diameter after 24 passes decreased to about half the size.

The smallest grains were mainly observed in the middle of the strip thickness. Their orientations are between <111> (Fig. 18). After CRCS process the number of lower angle grain boundaries increased, also with disorientation angle under 10° (Fig. 19).

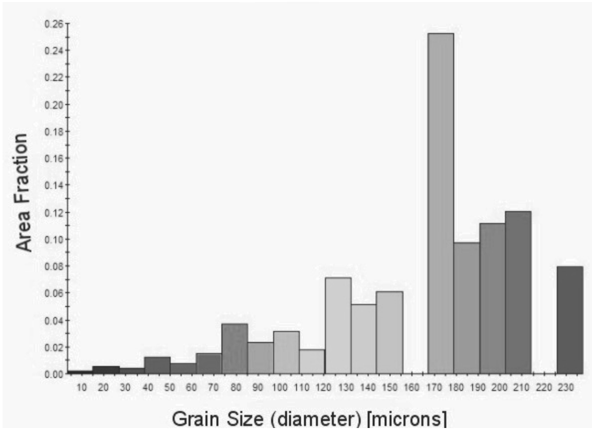

Fig. 12. Grain size distribution of initial quenched strip

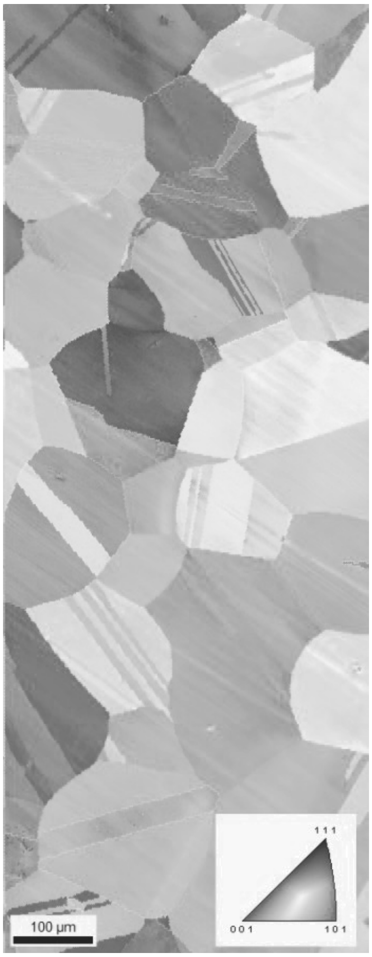

Fig. 13. Inverse Pole Figure (IPF) map of initial quenched strip

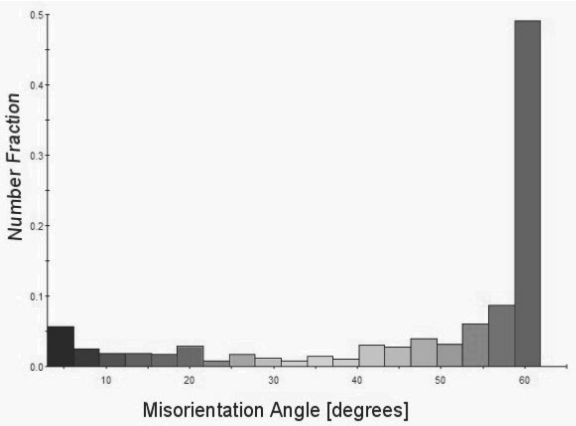

Fig. 14. Grain boundaries misorientation angle distribution of initial quenched strip

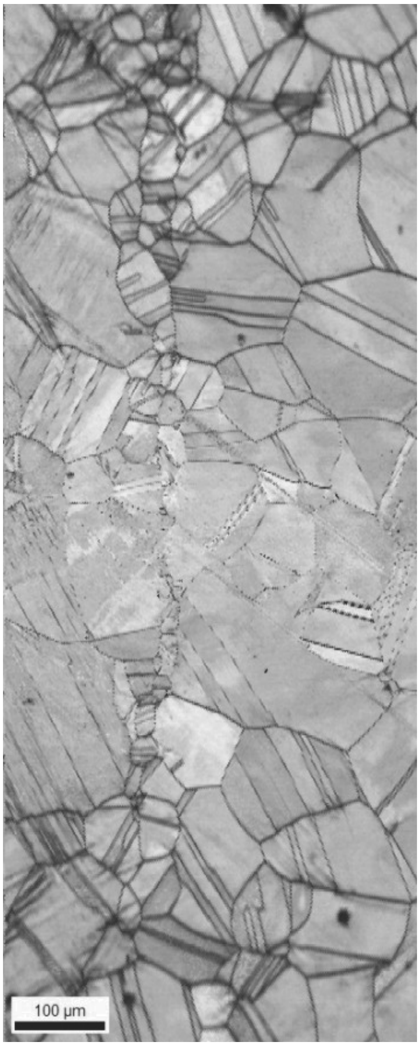

Fig. 15. Image quality map (IQ map) after CRCS process of initial quenched strip

Fig. 16. Grain map after CRCS process of initial quenched strip

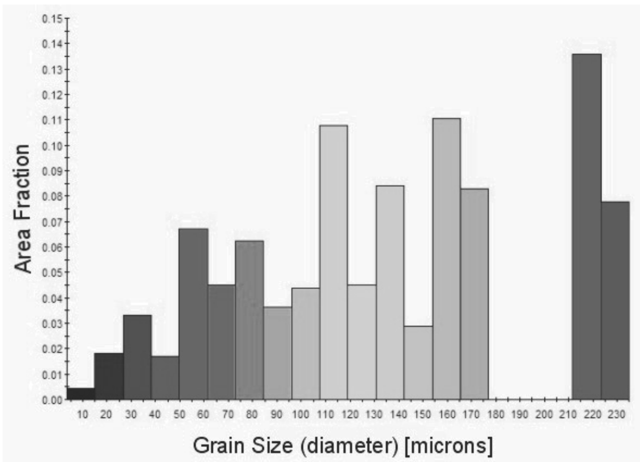

Fig. 17 Grain size distribution after CRCS process of initial quenched strip

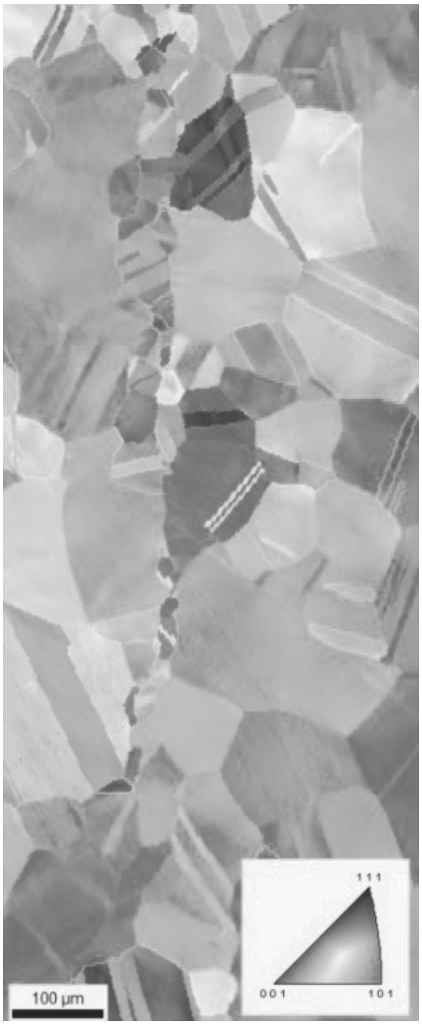

Fig. 18. Inverse Pole Figure (IPF) map after CRCS process of initial quenched strip

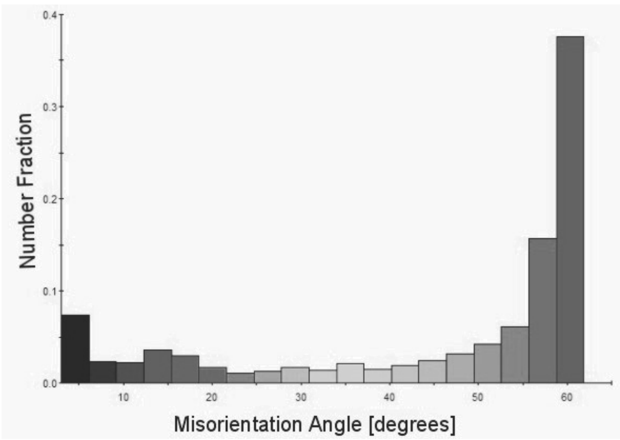

Fig. 19. Grain boundaries misorientation angle distribution after CRCS process of initial quenched strip

As it was mentioned before, the grain size, as predicted by EBSD data seems to be smaller than the actual value. To provide accuracy, these results were used in combination with TEM to determine the correct value. Figs. 20-21 show CuNi2Si1 TEM micrographs of initial and CRCS deformed samples. Microstructure (Fig. 20) of the quenched sample shows that it is completely supersaturated. There is no precipitation effect visible. During CRCS process inside the primary grains individual deformation twins and grains or sub-grains were produced, of sizes ranging from about 100 nm to a few hundred nanometres. Also many dislocation cells and arrays of dislocations were observed.

Fig. 20. Microstructure of initial (as quenched) sample

Similar sets of figures for annealed strips and CRCS processed after annealing are presented in Figs. 22-30, respectively.

In the annealed initial samples (Fig. 22) there are many precipitates of the Ni_2Si phase in the copper-rich matrix. In these areas dark spots are observed produced by not indexable Cu-EBSD patterns In this scan area about 85% of the surface was correctly indexed, therefore the fraction of the (dark spots) secondary phase is ~15%, twin fraction: 0.28 and fraction of twinned grains about 0.48.This value does not correspond directly to the quantity of Ni_2Si precipitates. Some etching effects around the precipitates are also visible. The measured average grain diameter was lower than 10 µm, (Fig. 23). The grains are rather randomly orientated (Fig. 24) and misorientation angles between adjacent grains are mainly of high angle (Fig. 25). The grain size in CRCS processed samples is very low. Average grain size diameter is about 2 µm and most of them are of high angle. Similarly to the initial state they are not preferably oriented.

Using transmission electron microscopy, presence of sub-grains smaller than100 nm was confirmed (Fig. 30).

a)

b)

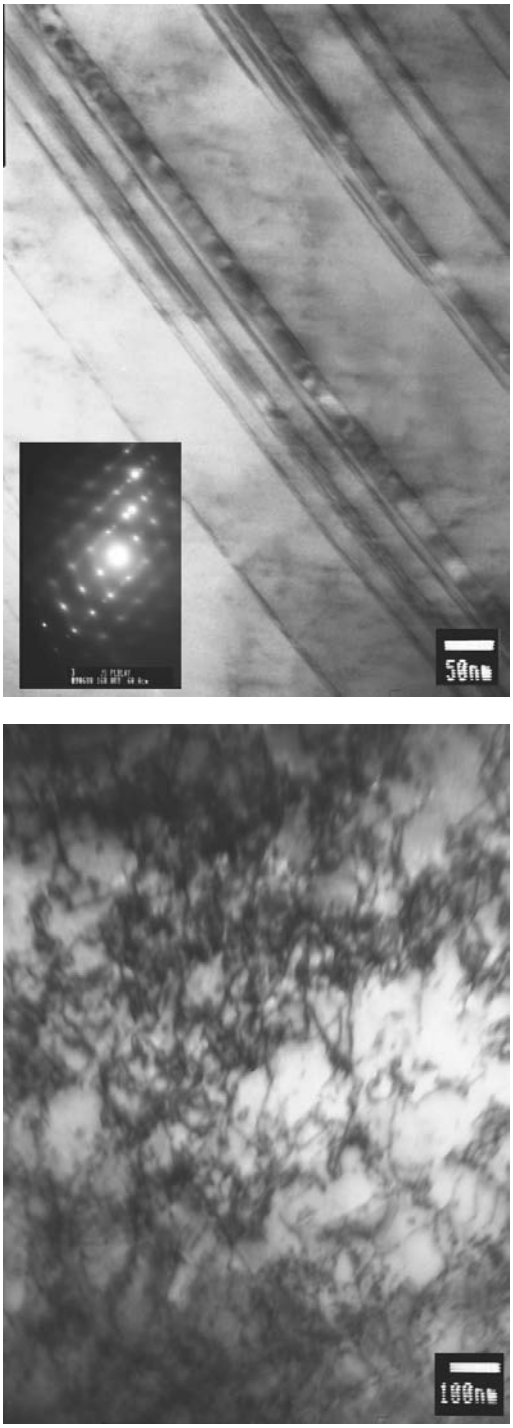

Fig. 21. Microstructure of CRCS processed sample; a) deformation twins and diffraction of zone axis [101] of matrix and twins b) ultrafine grained microstructure in areas between twins

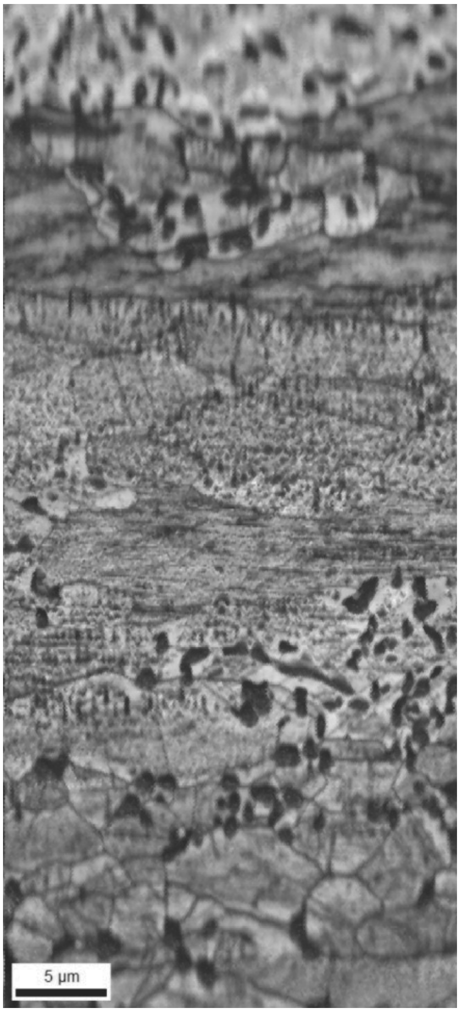

Fig. 22. Image quality map (IQ map) of annealed sample strip

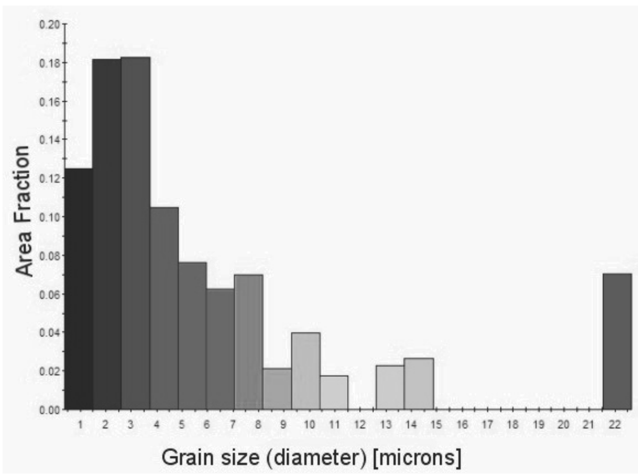

Fig. 23. Grain size distribution of annealed sample strip

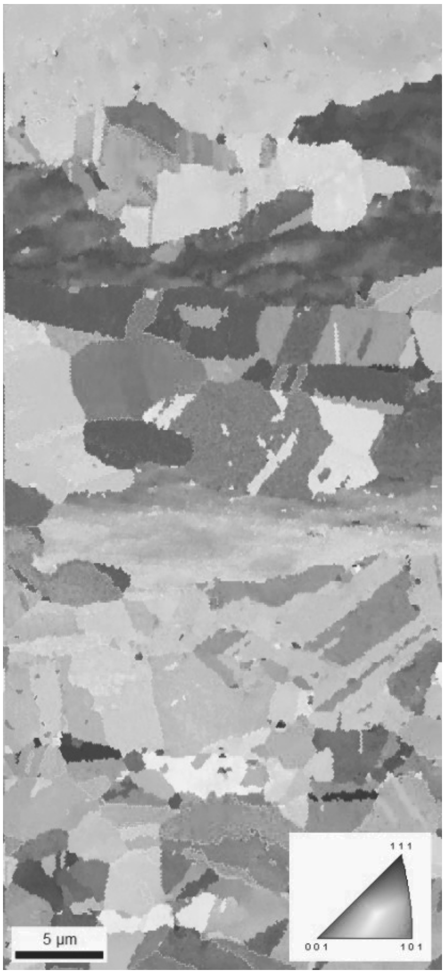

Fig. 24. Inverse Pole Figure (IPF) map of annealed sample strip

Fig. 26. Quality image map (IQ map) after CRCS processing of annealed sample strip

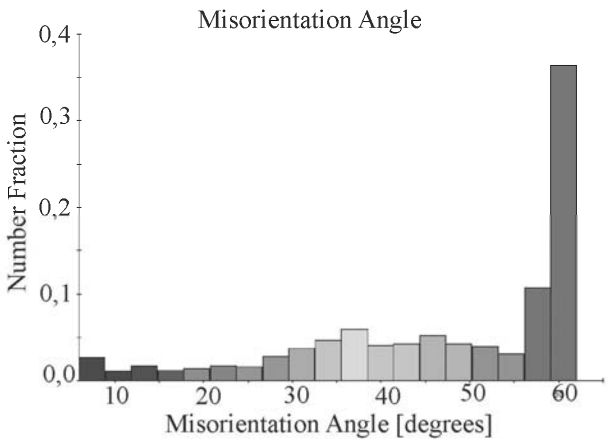

Fig. 25. Grain boundaries misorientation angle distribution of annealed sample strip

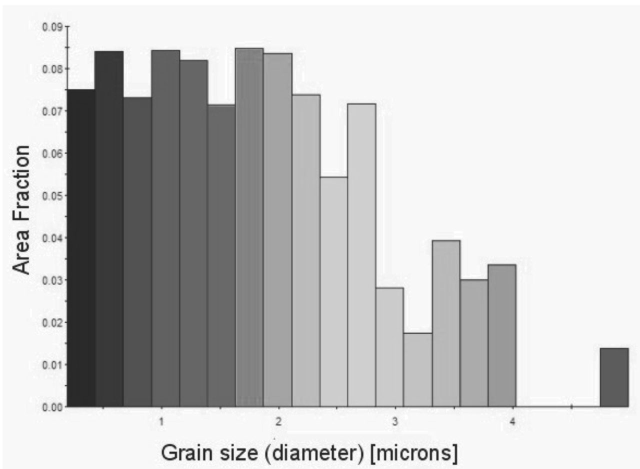

Fig. 27. Grain size distribution after CRCS process of annealed sample strip

Fig. 28. Inverse Pole Figure (IPF) map after CRCS process of annealed sample strip

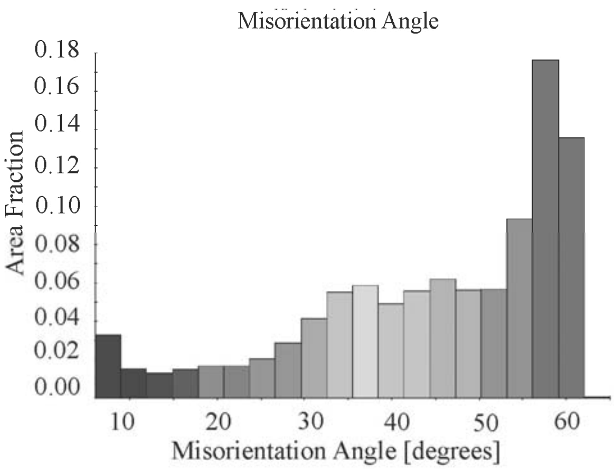

Fig. 29. Grain boundaries misorientation angle distribution after CRCS process of annealed sample strip

a)

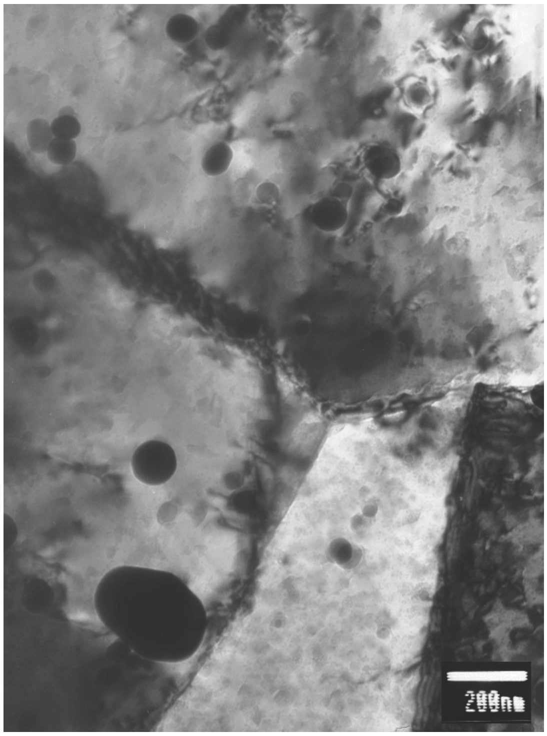

b)

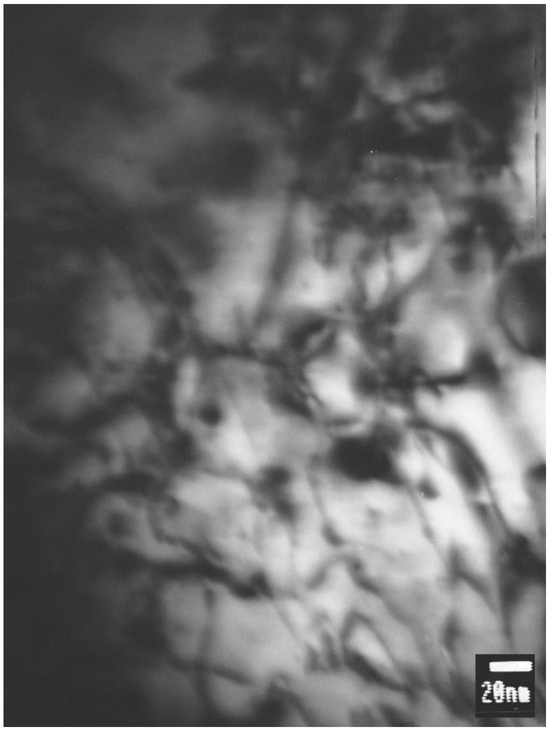

Fig. 30. Microstructure of CuNi2Si1 alloy strips: as annealed (a), after 34 passes of deformation; (b) TEM

6. Fracture

Figures 31-32 shows the fracture surfaces of the (a) initial and (b) CRCS processed samples after tensile test. At the bottom of the dimples the fractographs show holes which are nucleation sites for fracture.

There is no significant difference in the dimple size between the two fractographs (a and b), in spite of the significant difference in grain size. The differences are caused by inclusions (Ni_2Si particles) and precipitate distribution. The obtained results are comparable with those obtained by Mishra at al. [21-22] for copper. The similarity in the fracture morphology can be interpreted as resulting from the fact that the nucleation sites have similar distribution for both (initial and CRCS processed) conditions. The same distributions of these particles results in formation of dimples, regardless the grain size. Nevertheless, in the ultrafine-grained material the dimples seem to be shallower what is a direct consequence of the decreased ductility.

a)

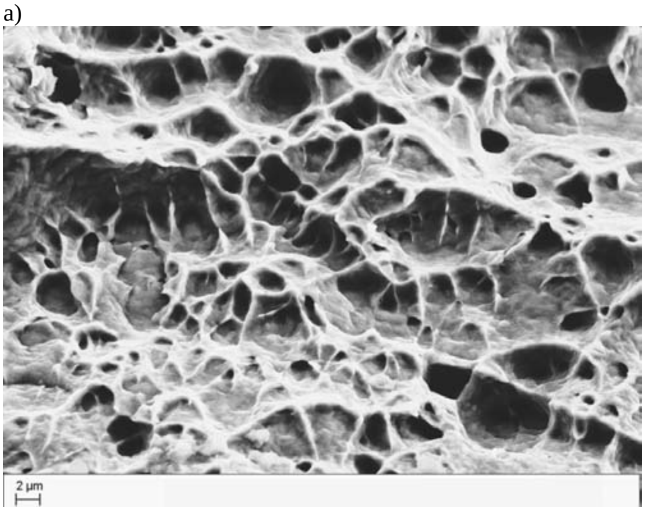

b)

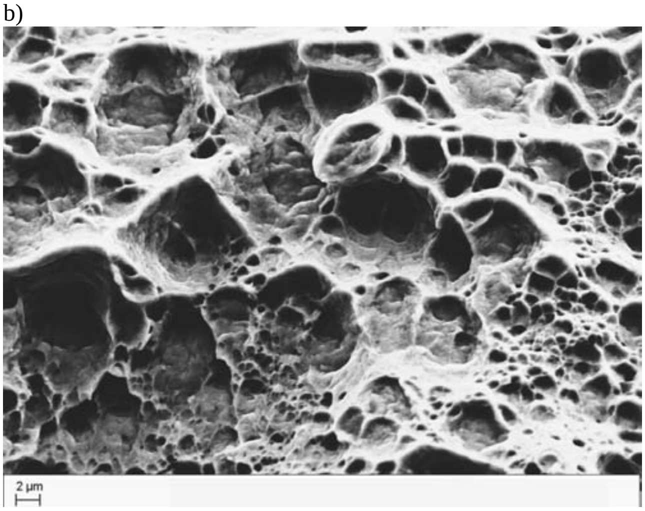

Fig. 31. SEM micrographs of fracture surface of $CuNi_2Si$ samples: (a) initial quenched and (b) after CRCS processing

a)

b)

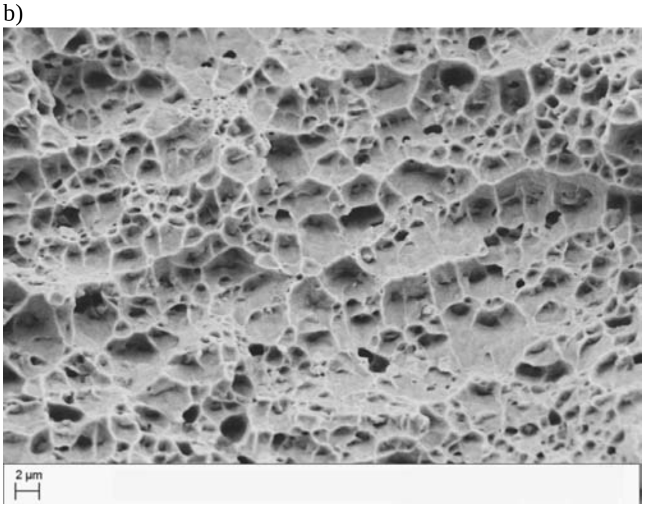

Fig. 32. SEM micrographs of fracture surface of $CuNi_2Si$ samples: (a) initial annealed and (b) after CRCS processing

7. Conclusions

This study was aimed to investigate mechanical properties and microstructure in CuNi2Si1 alloy strips processed by continuous repetitive corrugation and straightening (CRCS). Based on the obtained results, the following conclusions can be drawn:

- The CRCS process effectively reduced the grain size of the investigated strips, demonstrating the CRCS as a promising new method for producing ultra fine grained metallic strips;
- The sizes of structure elements revealed by OIM analysis were larger than those determined by TEM. TEM micrographs of the deformed microstructure showed that individual grains or sub-grains were produced inside the primary grains with sizes ranging from below 100 nm to a few

hundred nanometres. Also many dislocation cells and arrays of dislocations were observed;

- Effectiveness of grain size reduction is higher for the annealed samples, presence of strengthening Ni_2Si phase favours microstructure refining in all processing stages;
- The values of strength characteristics of investigated strips such as yield strength and ultimate tensile strength increased after CRCS (especially for quenched material) when compared to initial state and remain virtually constant in the deformation range over N=12 cycles. Further deformation increase caused decrease of strength.

Acknowledgements

This work was supported by the State Committee for Scientific Research under the projects No PBZ-MNiSW-3/3/2006 zad.4.1 and No N N507271836

References

[1] M. Greger, R. Kocich, L. Cizek, L.A. Dobrzański, M. Widomska, B. Kuretova, A. Silbernagel, The structure and properties of chosen metals after ECAP, Journal of Achievements in Materials and Manufacturing Engineering 18 (2006) 103-106.

[2] J. Stobrawa, Z. Rdzawski, Deformation behaviour of dispersion hardened nanocrystalline copper, Journal of Achievements in Materials and Manufacturing Engineering 17 (2006) 153-156.

[3] J. Stobrawa, Z. Rdzawski, W. Głuchowski, Structure and properties of dispersion hardened submicron grained copper, Journal of Achievements in Materials and Manufacturing Engineering 20 (2007) 195-198.

[4] J. Stobrawa, Z. Rdzawski, Dispersion – strengthened nanocrystalline copper, Journal of Achievements in Materials and Manufacturing Engineering 24/2 (2007) 35-42.

[5] J.P. Stobrawa, Z.M. Rdzawski, Microstructure and properties of nanocrystalline copper – yttria microcomposite, Journal of Achievements in Materials and Manufacturing Engineering 24/2 (2007) 83-86.

[6] J.P. Stobrawa, Z.M. Rdzawski, Thermal stability of functional properties in dispersion and precipitation hardened selected copper alloys, Archives of Materials Science and Engineering 30/1 (2008) 17-20.

[7] J.P. Stobrawa, Z.M. Rdzawski, Formation of a stable nanostructure n the copper-based materials, Proceedings of the 11th International Scientific Conference "Contemporary Achievements in Mechanics, Manufacturing and Materials Science" CAM3S'2005, Gliwice − Zakopane, 2005, 909-914.

[8] M. Greger, R. Kocich, L. Cizek, Grain refining of Cu and Ni-Ti shape memory alloys by ECAP process, Journal of Achievements in Materials and Manufacturing Engineering 20 (2007) 247-250.

[9] L. Cizek, M. Greger, L.A. Dobrzański, I. Juricka, R. Kocich, L. Pawlica, T. Tański, Structure and properties of alloys of the Mg-Al-Zn system, Journal of Achievements in Materials and Manufacturing Engineering 32/2 (2009) 179-187.

[10] S. Rusz, K. Malanik, Refining of structure of the alloy AlMn1Cu with use of multiple severe plastic deformation, Journal of Achievements in Materials and Manufacturing Engineering 27/2 (2008) 167-170.

[11] S. Rusz, K. Malanik, J. Dutkiewicz, L. Cizek, I. Skotnicova, J. Hluchnik, Influence of change of direction of deformation at ECAP technology on achieved UFG In AlMn1Cu alloy, Journal of Achievements in Materials and Manufacturing Engineering 35/1 (2009) 21-28.

[12] Il Heon Son, Young Gwan Jin, Jeong Ho Lee, Young-Taek Im, Load predictions for non-isothermal ECAE by finite element analyses, International Journal of Computational Materials Science and Surface Engineering 1/2 (2007) 242-258.

[13] M. Kulczyk, W. Pachla, A. Mazur, M. Suś-Ryszkowska, N. Krasilnikov, K.J. Kurzydłowski, Producing bulk nanocrystalline materials by combined hydrostatic extrusion and equal-channel angular pressing, Materials Science-Poland 25/4 (2007) 991-999.

[14] Y.H. Zhao, X.Z. Liao, Y.T. Zhu, Z. Horita, T.G. Langdon, Influence of stacking fault energy on nanostructure formation under high pressure torsion, Materials Science and Engineering A 410-411 (2005) 188-193.

[15] X. Sauvage, R. Pippan, Nanoscaled structure of a Cu-Fe composite processed by high-pressure torsion, Materials Science and Engineering A 410-411 (2005) 345-347.

[16] Y.H. Zhao, Y.T. Zhu, X.Z. Liao, Z. Horita, T.G. Langdon, Influence of stacking fault energy on the minimum grain size achieved in severe plastic deformation torsion, Materials Science and Engineering A 463 (2007) 22-26.

[17] K. Rodak, Severely deformed Cu by using compression with oscillatory torsion method, Journal of Achievements in Materials and Manufacturing Engineering 20 (2007) 179-182.

[18] Y.T. Zhu, H. Jiang, T.C. Love, A new route to bulk nanostructured materials, Metallurgical and Materials Transactions A: Physical Metallurgy and Materials Science 32/6 (2001) 1559-1562.

[19] J.Y. Huang, Y.T. Zhu, H. Jiang, T.C. Love, Microstructure and dislocation configuration in nanostructured Cu processed by repetitive corrugation and straightening, Acta Materialia 49 (2001) 1497-1505.

[20] J. Huang, Y.T. Zhu, D.J. Alexander, X. Liao, T.C. Love, R.J. Asaro, Development of repetitive corrugation and straightening, Materials Science and Engineering A 371 (2004) 35-39.

[21] A. Mishra, V. Richard, F. Gregori, R.J. Asaro, M.A. Meyers, Microstructural evolution in copper processed by severe plastic deformation, Materials Science and Engineering A 410-411 (2005) 290-298.

[22] A. Mishra, B.K. Kad, F. Gregori, M.A. Meyers, Microstructural evolution in copper subjected to severe plastic deformation: Experiments and analysis, Acta Materialia 55 (2007) 13-28.